

# A Method for Reduction of Numerical Diffusion in the Donor Cell Treatment of Convection

KANG Y. HUH, MICHAEL W. GOLAY, AND VINCENT P. MANNO

*Department of Nuclear Engineering, Massachusetts Institute of Technology,  
Cambridge, Massachusetts 02139*

Received April 26, 1984; revised May 6, 1985

This article is concerned with the donor cell treatment of convection in numerical simulations of convective–diffusive flow. The two sources of numerical diffusion in this treatment, truncation error and crossflow diffusion, are explained and quantified. Truncation error occurs due to the use of approximate profile assumptions while crossflow diffusion arises due to cell-wise homogenization of the convected quantity in multidimensional problems. Crossflow diffusion is the dominant source of error in many cases. A corrective scheme is introduced in this article which compensates for the effect of crossflow diffusion by reducing the effective anisotropic diffusion coefficient used in the diffusion portion of the simulation. Relationships are developed quantifying the crossflow diffusional error and requirements for explicit numerical stability when the error correction technique is employed. The magnitudes of the diffusional error and the improvements realized using the corrective scheme are demonstrated through computational examples. © 1986 Academic Press, Inc.

## 1. INTRODUCTION

Numerical diffusion arising in the use of the donor cell treatment of convection continues to be a source of confusion and difficulty in the field of computational fluid dynamics. The purpose of this article is to clarify and quantify the sources of numerical diffusion in the donor cell treatment of convection–diffusion problems, and to suggest a method for correction of crossflow diffusion. Numerical diffusion comes from two different sources: truncation error and crossflow diffusion. Truncation error arises from use of approximate profile assumptions in infinitesimally differencing temporal and spatial derivative terms while crossflow diffusion arises from cell-wise homogenization of the convected quantity in a multidimensional problem. Crossflow diffusion is found to be the dominant source of error in many problems. In this article the crossflow diffusion error is quantified and a scheme for its reduction is proposed. The stability conditions for the new corrective scheme are derived by the von Neumann method in terms of the dimensionless numbers,  $u \Delta t / \Delta x$  and  $u \Delta x / D$ . Validation calculations are performed in a simple geometry so that the numerical solutions can be compared easily with corresponding analytic solutions. Finally, the corrective scheme is applied to the test problem presented in [12].

## 2. TRUNCATION ERROR DIFFUSION

Truncation error occurs due to the approximate nature of a finite difference equation and usually appears as additional diffusion. Most previous analyses (e.g., [5, 6, 11]) have concentrated on the evaluation of this source of inaccuracy. A finite difference equation is derived from a partial differential equation by using assumed profiles for the spatial and temporal variation of the quantity under consideration. Since these profiles are not generally exact, truncation errors are unavoidable. However, it is possible to reduce such errors to an acceptable level by assuming reasonable profiles based upon appropriate dimensionless numbers and using weighted differencing schemes [8]. For example, along the inflow boundary of a cell it is reasonable to assume that a local upstream value prevails (i.e., a uniform profile) when convection is dominant over diffusion or that a profile is locally linear when diffusion is dominant over convection [13].

The profile of a general conserved quantity  $\phi$  is given by the dimensionless cell Peclet number,  $P = u \Delta x / D$ . Its value indicates the relative importance of convection and diffusion. The name, truncation error, originates from the truncation of the second- and higher-order terms in the derivation of a finite difference equation as with the example

$$\left(\frac{\partial\phi}{\partial x}\right)_n = \frac{\phi_{i+1} - \phi_i}{\Delta x} - \frac{\Delta x}{2} \left(\frac{\partial^2\phi}{\partial x^2}\right)_i + \frac{\Delta x^2}{6} \left(\frac{\partial^3\phi}{\partial x^3}\right)_i - \dots \simeq \frac{\phi_{i+1} - \phi_i}{\Delta x}. \quad (1)$$

The approximation in Eq. (1) is valid if the profile of  $\phi$  is almost linear over  $\Delta x$  such that

$$\frac{(\Delta x)^{n-1}}{n!} \frac{\partial^n \phi}{\partial x^n} \simeq 0 \quad \text{for } n \geq 2. \quad (2)$$

Since truncation error arises both in one-dimensional and multidimensional problems a one-dimensional case is chosen for analysis for the sake of clarity. In an illustration to quantify the truncation error, an analytical solution and a numerical solution is obtained for a steady-state one-dimensional convection-diffusion case with no source and are compared to each other to obtain the effective diffusion term which is introduced into the numerical solution by this error. The results of the analysis may be extended to a general one-dimensional case if the effects of the transient and source terms are not dominant in determining the profile of  $\phi$ . The governing equation is

$$u \frac{\partial\phi}{\partial x} = D \frac{\partial^2\phi}{\partial x^2}. \quad (3)$$

The calculation domain of length  $L$  is divided into  $N$  equal cells with a cell interval  $\Delta x = L/N$ . The two boundary values  $\phi(x=0) = \phi_0$  and  $\phi(x=L) = \phi_N$  are assumed to be known constants. The analytical solution to Eq. (3) is

$$\phi = C_1 e^{cx} + C_2, \quad (4)$$

where

$$c = u/D, \quad C_1 = (\phi_N - \phi_0)/(e^{cL} - 1), \\ C_2 = (\phi_0 e^{cL} - \phi_N)/(e^{cL} - 1), \quad \text{and it is assumed that } u \geq 0.$$

Equation (3) is finitely differenced using the donor cell and central difference schemes for the convection and diffusion terms, respectively, as

$$u \frac{\phi_i - \phi_{i-1}}{\Delta x} = D \frac{\phi_{i+1} - 2\phi_i + \phi_{i-1}}{\Delta x^2}, \quad (5)$$

where it is assumed  $u \geq 0$ . Equation (5) can be stated as

$$P(\phi_i - \phi_{i-1}) = \phi_{i+1} - 2\phi_i + \phi_{i-1}. \quad (6)$$

The solution to Eq. (6) is given by the relationship

$$\phi_i = \phi_0 + \frac{(1+P)^i - 1}{(1+P)^N - 1} (\phi_N - \phi_0). \quad (7)$$

By substitution of both the analytical and numerical solutions into the diffusion term of Eq. (5), the effective diffusion coefficient for the numerical solution can be obtained. The resulting relationships

$$\phi_{i+1} - 2\phi_i + \phi_{i-1} = \frac{e^{(i-1)P}}{e^{NP} - 1} (e^P - 1)^2 (\phi_N - \phi_0) \quad (8)$$

and

$$\phi_{i+1} - 2\phi_i + \phi_{i+1} = \frac{(1+P)^{i-1} P^2}{(1+P)^N - 1} (\phi_N - \phi_0) \quad (9)$$

are obtained using the analytic and numerical solutions, respectively. Comparison of

Eqs. (8) and (9) allows the formulation of an effective cell Peclet number  $P_e$  which governs the numerical solution in terms of the actual cell Peclet number  $P$  as

$$\frac{e^{(i-1)P_e}}{e^{NP_e}-1} (e^{P_e}-1)^2 = \frac{(1+P)^{i-1} P^2}{(1+P)^N-1}, \quad (10)$$

where  $P_e = u \Delta x / D_e$ , and  $D_e$  is the effective (i.e., numerical plus physical) diffusion coefficient which is reflected in the numerical solution. Equation (10) can be reduced to the form

$$P_e = \ln(1+P). \quad (11)$$

Table I shows for this case that the ratio of the truncation error diffusion constant to the physical diffusion constant,  $D_{TE}/D$  is small for small values of  $P$ . It is also insignificant for large values of  $P$  in comparison to the crossflow diffusion constant which is the order of  $u \Delta x$  when the flow is not oriented with the grid in a multidimensional problem. Consequently, the error due to truncation error diffusion can be neglected in both diffusion-dominant and convection-dominant problems. It is illustrated in Section 6 that truncation error diffusion is tolerably small in many convection-diffusion problems.

Using the central difference treatment of convection,

$$u \frac{\phi_{i+1} - \phi_{i-1}}{2 \Delta x} = D \frac{\phi_{i+1} - 2\phi_i + \phi_{i-1}}{\Delta x^2}, \quad (12)$$

TABLE I

Dependence upon  $P$  of the Ratio of the Truncation Error Diffusion Constant to Physical Diffusion Constant and  $u \Delta x$  according to Eq. (11) ( $D_{TE} = D_e - D$ )

$P$	$D_{TE}/u \Delta x$	$D_{TE}/D$
0.1	0.49	0.05
0.2	0.48	0.10
0.5	0.47	0.23
1.0	0.44	0.44
2.0	0.41	0.82
5.0	0.36	1.79
10.0	0.32	3.17
100.0	0.21	20.67
1000.0	0.14	143.74
$10^8$	0.05	$4.38 \times 10^7$

the effective Peclet number for the finite difference solution of Eq. (12) is similarly found to be

$$P_e = \ln \left( \frac{2+P}{2-P} \right), \quad (13)$$

where  $-2 < P < 2$ .

### 3. CROSSFLOW DIFFUSION

The origins of crossflow diffusion have been identified by Patankar [7] and Stubbley *et al.* [14, 15] and it was argued that this is the dominant error source in most multidimensional convection-diffusion problems. In this section the origin of crossflow diffusion is illustrated and the corresponding diffusion constant is quantified so that it can be used in a corrective scheme. Other investigators have attempted to do this. For example, deVahl Davis and Mallinson [3] have attempted to quantify crossflow diffusion and suggested the following two-dimensional expression:

$$D_{DM} = \frac{U \Delta x \Delta y \sin^2 \theta}{4(\Delta y \sin^3 \theta + \Delta x \cos^3 \theta)}, \quad (14)$$

where  $U$  is the absolute magnitude of the velocity and  $\theta$  is the angle between the velocity vector and the  $x$  axis.

In analyzing and testing Eq. (14), we have found that it is valid only when  $\theta = \pi/4$  and  $\Delta x = \Delta y$  in a two-dimensional case, and that it usually underpredicts the crossflow diffusion effect.

The origin of crossflow diffusion is illustrated in Fig. 1 which shows a single cell used in describing a pure convection problem. In Fig. 1A hot and cold fluid enters the grid from the left and bottom surfaces, respectively, with their interface aligned

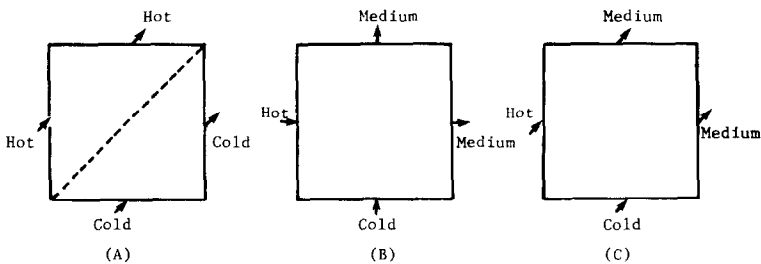
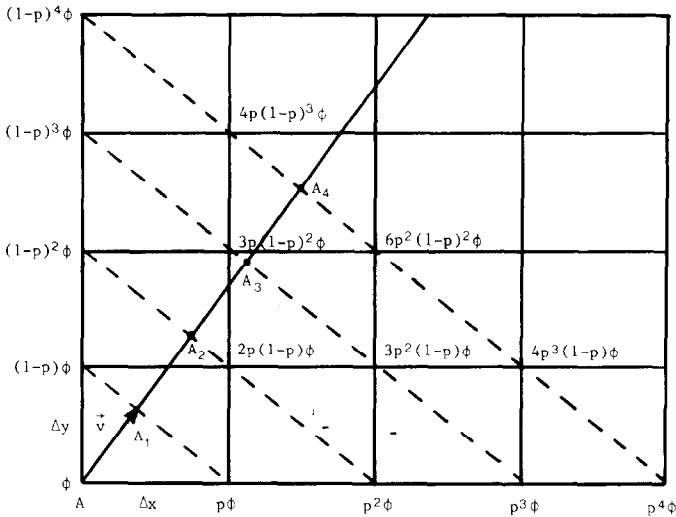


FIG. 1. Illustration of crossflow diffusion in a single cell for a purely convective flow oriented diagonally across the cell, with a hot-cold fluid interface crossing the cell diagonally: (1A) physical flow, (1B) donor cell treatment of that flow, (1C) resultant donor cell flow field.

at a 45° angle. In a flow without diffusion the hot fluid will issue from the top surface and the cold fluid from the right surface. The donor cell treatment of this flow is illustrated in Fig. 1B. Note that this treatment is formulated only in terms of velocity components normal to the cell surfaces. Homogeneous mixing of the inward flowing streams occurs within the mesh and intermediate temperature fluid will exit equally from the top and right surfaces. The numerical result outlined in Fig. 1B is interpreted physically as that shown in Fig. 1C. The homogenization illustrated in this example is the source of crossflow diffusion which arises independently of truncation error diffusion. It occurs only when the velocity field is not aligned with the grid.

The diffusive nature of this error is illustrated in the flow shown in Fig. 2 which shows an array of cells equally spaced, aligned in two dimensions, and used to describe a pure convection problem. In this flow the fluid is convecting the quantity  $\phi$  along the streamline passing through the origin of the coordinate system  $A$ , and  $\phi$  observed at point  $A$  should also be seen at points  $A_1, A_2, A_3,$  and  $A_4$ . However, in the donor cell treatment of convection  $\phi$  is distributed as shown in Fig. 2. It is seen along each plane intersecting the mesh points diagonally that  $\phi$  is conserved. For example, at the downstream diagonal level passing through the point  $A_3$  it is seen that the values at the mesh points add to  $\phi$  as

$$p^3\phi + 3p^2(1-p)\phi + 3p(1-p)^2\phi + (1-p)^3\phi = \phi. \tag{15}$$



$$\text{where } p = \frac{u/\Delta x}{u/\Delta x + v/\Delta y}$$

FIG. 2. Illustration of crossflow diffusion from the donor cell treatment of a purely convective flow in two dimensions.

The effective crossflow diffusion coefficient is obtained in the following discussion in two dimensions, utilizing the geometry of Fig. 2. During the time  $\delta t$  required for flow along the streamline from point  $A$  to  $A_1$  there occurs an  $x$ -directed transport of  $p\phi$  to the coordinate  $(\Delta x, 0)$  and the  $y$ -directed transport of  $(1-p)\phi$  to the coordinate  $(0, \Delta y)$ . The  $x$ -directed transport of  $p\phi$  occurs at a total velocity equal to  $\Delta x/\delta t$ , which is the sum of convective and diffusive contributions. The effective  $x$ -directed diffusive velocity is then obtained as:

$$u_{CF} = \frac{\Delta x}{\delta t} - u. \quad (16a)$$

Similarly, the  $y$ -directed effective diffusive velocity is obtained as

$$v_{CF} = \frac{\Delta y}{\delta t} - v. \quad (16b)$$

The effective  $x$ -directed and  $y$ -directed crossflow diffusion coefficients are defined, respectively, by the relationships:

$$-D_{CF} \frac{\partial \phi}{\partial x} = \ddot{\phi}_x \quad (17a)$$

and

$$-D_{CF} \frac{\partial \phi}{\partial y} = \ddot{\phi}_y. \quad (17b)$$

The  $x$ - and  $y$ -directed diffusive currents of  $\phi$  are obtained, respectively, as

$$\ddot{\phi}_x = u_{CF} p\phi \quad (18a)$$

and

$$\ddot{\phi}_y = v_{CF}(1-p)\phi. \quad (18b)$$

The gradients of  $\phi$  may be approximated as follows:

$$\frac{\partial \phi}{\partial x} \approx -\frac{\phi}{\Delta x} \quad (19a)$$

and

$$\frac{\partial \phi}{\partial y} \approx -\frac{\phi}{\Delta y}. \quad (19b)$$

From Eq. (17) the respective diffusion coefficients are then obtained as

$$D_{CF_x} = p \Delta x u_{CF} \quad (20a)$$

and

$$D_{CF_y} = (1 - p) \Delta y v_{CF}. \quad (20b)$$

From geometrical considerations  $\delta t$  is obtained as:

$$\delta t = \left( \frac{u}{\Delta x} + \frac{v}{\Delta y} \right)^{-1}. \quad (21)$$

Note that the streamline is not required to be orthogonal to the cross-grid diagonal from the coordinates  $(\Delta x, 0)$  to  $(0, \Delta y)$  to obtain these results.

Utilizing Eqs. (16) and (21) the respective  $x$ - and  $y$ -directed diffusion coefficients are obtained in the form:

$$D_{CF_x} = u \Delta x [1 - p] \quad (22a)$$

and

$$D_{CF_y} = v \Delta y p. \quad (22b)$$

The three-dimensional extension of this result is

$$D_{CF_x} = u \Delta x (1 - p_x), \quad (23a)$$

$$D_{CF_y} = v \Delta y (1 - p_y) \quad (23b)$$

and

$$D_{CF_z} = w \Delta z (1 - p_z). \quad (23c)$$

#### 4. POSSIBLE DIFFUSION-MITIGATION METHODS: SKEW DIFFERENCING AND CORRECTIVE SCHEMES

Many schemes have been proposed to eliminate numerical diffusion. Among the most important ones are Raithby's scheme [9], the tensor viscosity method [4], the finite element method [1], and method of characteristics [2]. Most of these schemes can be categorized into two classes: skew upwind differencing and donor cell corrective schemes. In a skew differencing scheme, finite upwind differencing of the convection term is performed not in terms of the mesh direction velocity com-



ponents, but along the velocity vector direction. While the donor cell treatment of the convection term results in a 5-point relationship in a two-dimensional problem, the skew differencing scheme involves a 9-point relationship. The inclusion of four additional corner points contributes to more accurate numerical modeling of convection. However, unphysical results may arise because of deviations of the flow streamlines from the linear interpolation path used in the skew differencing scheme in convection-dominant problems.

The tensor viscosity method is similar to that of this work in that it provides a convective directionally dependent diffusivity to compensate for negatively diffusive truncation errors arising in the central-differencing treatment of transient convection. In the case of the tensor viscosity method the compensation consists of both truncation and crossflow positive diffusivities added to the physical diffusivity.

Corrective schemes attempt to reduce the effective diffusion constant operating in a problem to compensate for the effect of the additional donor cell-induced numerical diffusion. However, such schemes are valid only when the effective numerical diffusion constants can be predicted accurately. Since crossflow diffusion is the dominant error source in many multidimensional problems (see Sect. 6), and its effective diffusion coefficients for crossflow diffusion can be predicted theoretically, the corrective scheme could be expected to provide a numerical solution which is almost free from numerical diffusion error.

#### *A New Corrective Scheme*

The corrective scheme proposed in this paper uses the directionally dependent diffusion coefficients defined in Eq. (23) to reduce diffusion currents of  $\phi$  in the  $x$ ,  $y$ , and  $z$  directions. The physical diffusion coefficient  $D_{\text{ph}}$  is defined at a cell center and the crossflow diffusion constant,  $D_{\text{CF}_x}$ ,  $D_{\text{CF}_y}$ , or  $D_{\text{CF}_z}$  is defined at a cell interface, and is dependent upon the local velocity vector. Using the proposed corrective scheme the effective value of  $D$  in Eq. (24) is calculated as  $D_{\text{ph}} - D_{\text{CF}_x}$  for  $x$ -directed diffusion, and by  $D_{\text{ph}} - D_{\text{CF}_y}$  for  $y$ -directed diffusion.

The implementation of Eq. (23) in a practical problem must be considered carefully. All of the two-dimensional results reported here are obtained using a staggered grid, where the two outward normal velocity components  $u$  and  $v$  are used with the cell dimensions to calculate the crossflow diffusion coefficients. These coefficients are assigned to each of the cell faces to reduce their respective diffusional currents. Since velocity vectors should be used in making these diffusional corrections, a degree of unavoidable arbitrariness arises in cases where the velocity field is not uniform over a single cell and some interpolation formula must be used in defining the velocity vector characteristic of each cell face.

It is also important to note that this convective scheme does not account for all numerical errors. For example, when the velocity is oriented at  $45^\circ$  to the  $x$  axis the corrective scheme becomes identical to the central difference scheme. The latter has been shown to include significant errors in addition to those of crossflow diffusion [14].

## 5. STABILITY OF THE PROPOSED CORRECTIVE SCHEME

In the proposed corrective scheme the physical diffusion coefficient is reduced to compensate for crossflow diffusion. When the magnitude of the physical diffusion coefficient is less than that for crossflow diffusion, the value of  $(D_{ph} - D_{CF})$  becomes negative. To our knowledge, the stability of a finite difference equation with a negative diffusion constant has not been treated in the literature, but must be given careful consideration here since it is vital to the generally successful application of the corrective scheme. In this section the stability conditions of this scheme are derived by the von Neumann method in terms of the dimensionless numbers,  $C_x = u \Delta t / \Delta x$ ,  $d_x = D \Delta t / \Delta x^2$ , and  $P_x = u \Delta x / D$ .

A two-dimensional convection-diffusion equation in an explicit donor-cell convection, central-difference diffusion form is given as

$$\begin{aligned} & \frac{\phi_{ij}^{n+1} - \phi_{ij}^n}{\Delta t} + u \frac{\phi_{ij}^n - \phi_{i-1j}^n}{\Delta x} + v \frac{\phi_{ij}^n - \phi_{ij-1}^n}{\Delta y} \\ & = D \frac{\phi_{i+1j}^n - 2\phi_{ij}^n + \phi_{i-1j}^n}{\Delta x^2} + D \frac{\phi_{ij+1}^n - 2\phi_{ij}^n + \phi_{ij-1}^n}{\Delta y^2} \end{aligned} \quad (24)$$

assuming  $u$  and  $v$  are positive. The solution  $\phi_{ij}^n$  is expanded in the von Neumann method as

$$\phi_{ij}^n = \sum \zeta^n e^{I(i\theta_x + j\theta_y)}, \quad (25)$$

where  $I = \sqrt{-1}$ .

Substitution of Eq. (25) into Eq. (24) yields the following expression for the amplification factor  $\zeta$ , the absolute value of which should be less than unity to guarantee stability, or

$$\zeta = 1 - C_x(1 - e^{-I\theta_x}) - C_y(1 - e^{-I\theta_y}) - 2d_x(1 - \cos \theta_x) - 2d_y(1 - \cos \theta_y), \quad (26)$$

where

$$\begin{aligned} C_x &= \frac{u \Delta t}{\Delta x}, & d_x &= \frac{D \Delta t}{\Delta x^2}, \\ C_y &= \frac{v \Delta t}{\Delta y}, & d_y &= \frac{D \Delta t}{\Delta y^2}, \end{aligned}$$

and

$$|\zeta| \leq 1 \quad \text{for stability.} \quad (27)$$

The Courant numbers,  $C_x$  and  $C_y$  are defined such that they are always positive, regardless of the directions of the velocities  $u$  and  $v$ . The stability conditions can be

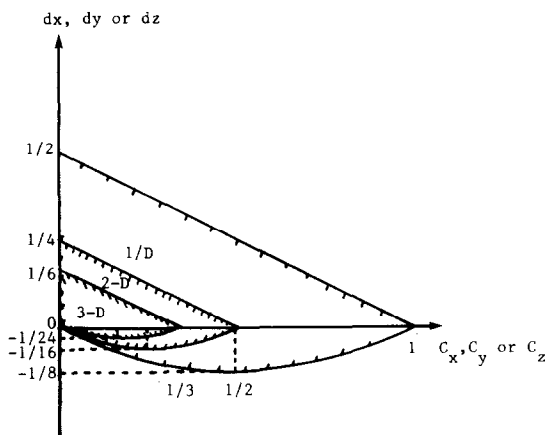


FIG. 3. Domain of stability of Eq. (24) in the plane  $(C_x, d_x)$ , etc., for explicit scheme with donor cell differencing of convection term in one-, two-, and three-dimensional cases, respectively.

derived from Eq. (28) in terms of  $C_x, C_y, d_x,$  and  $d_y$  by a graphical method using the characteristics of a quadratic equation. Although the details of the algebra are not presented here, the resulting domain of stability in  $(C, d)$ -space is illustrated in Fig. 3. The stability conditions for one-, two-, and three-dimensional cases are illustrated in Fig. 3, which shows that the size of the stable region in  $(C, d)$ -space shrinks on a linear scale with increasing dimensionality. This dependency has not been identified by other investigators [6, 10].

Since our usual concern is the determination of the maximum stable time-step size for a given mesh spacing, it is necessary to specify the stable range of  $C_x$  for a given cell Peclet number  $u \Delta x/D = P_x$ , which is independent of the time-step size. The stability condition for the finite difference equation, Eq. (24) is given in terms of  $C_x$  and  $P_x$  in Fig. 4. Finally, Table II contains a comparison of numerical

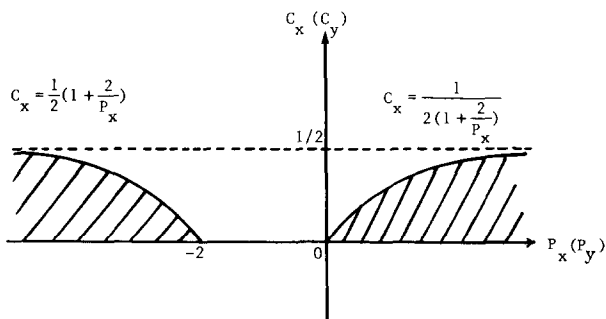


FIG. 4. Stability domain in the  $(P_x, C_x)$  and  $(P_y, C_y)$  planes, respectively, for the explicit scheme with donor cell differencing of the convective term (Eq. (24)) in a general two-dimensional problem.

TABLE II

Comparison of the Stability Conditions in Terms of the Cell Peclet Number by von Neumann Analysis to Results of Numerical Experiments. Equation (24) is Used to Obtain the Flow Field in the Problem Illustrated in Fig. 6B.

$P_x$	Maximum stable $C_x$	
	Von Neumann analysis	Numerical experiments
0.833	0.147	0.180
8.333	0.403	0.540
83.333	0.488	0.660
833.3	0.499	0.660
-8.333	0.499	0.660
-4.167	0.260	0.720
-2.629	0.120	0.120
-2.083	0.019	0.060

experimental results to the stability condition presented in Fig. 4. The case examined is that shown in Fig. 6B, using both positive and negative diffusion coefficients. The von Neumann analysis is shown to be qualitatively correct and uniformly to underestimate the maximum stable time step size which actually obtains. The domain of stability of the fully implicit version of Eq. (24) has also been determined from a similar von Neumann analysis to be

$$P_x < -2, \quad P_x > 0, \quad \text{and} \quad C_x > 0. \quad (28)$$

## 6. RESULTS

Illustration of crossflow diffusion being much greater than truncation error diffusion:

Truncation error and crossflow diffusion are compared in the flow geometry of Fig. 5 where an analytical solution for the steady convection diffusion-determined distribution of  $\phi$  at the domain exit can be obtained. In this case a uniform horizontal flow with an inlet boundary discontinuity in  $\phi$  is analyzed. The transport of  $\phi$  is governed by Eq. (29). Numerical solutions are obtained by donor cell differencing of the convection term and central differencing of the diffusive term. The equation for  $\phi$ -transport is governed by

$$u \frac{\partial \phi}{\partial x} = \alpha \left( \frac{\partial^2 \phi}{\partial x^2} + \frac{\partial^2 \phi}{\partial y^2} \right). \quad (29)$$

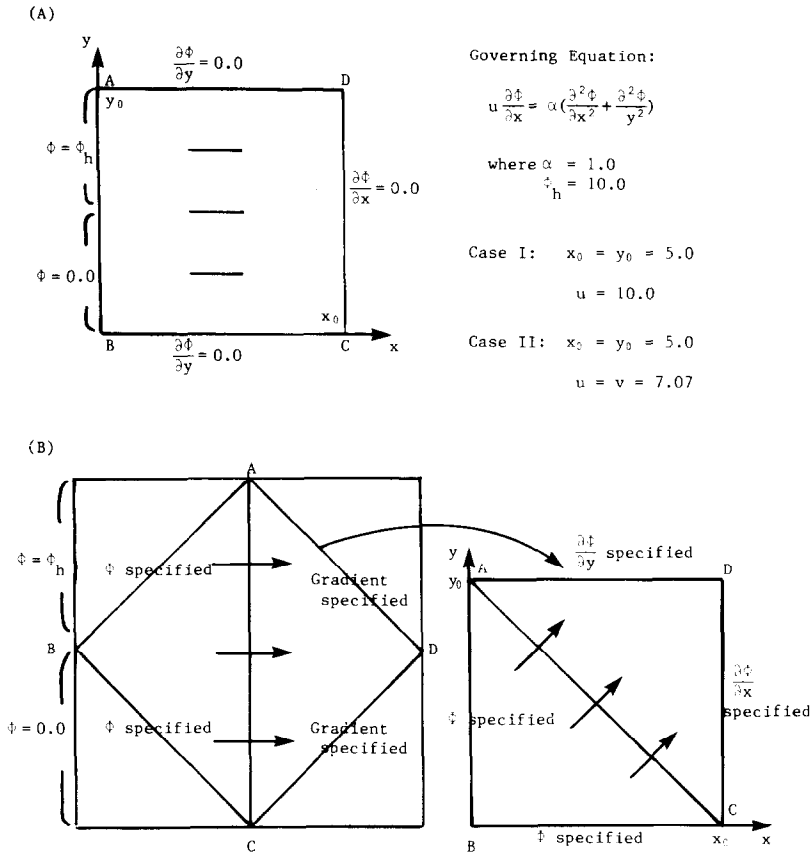


FIG. 5. Problem geometry for the two treatments of identical flow problems: (A) flow parallel to grid axis and (B) flow across the grid, in order to evaluate the magnitude of the crossflow diffusion coefficient.

This equation is solved as illustrated in Fig. 5. In one solution the numerical grid is aligned with the flow as shown in Fig. 5A, and in the other it is solved in a grid array aligned at  $45^\circ$  with the flow (see Fig. 5B). In both solutions both truncation and crossflow diffusion errors are included in the solution. In Fig. 6 the  $\phi$ -distribution results along selected lines in the domain are displayed. The results in Fig. 6A show that the numerical solution obtained using the grid alignment of Fig. 5A is close to the analytical solution and truncation error is negligible. Since truncation error diffusion occurs in the flow direction in this case, the numerical solution should give a steeper profile than the analytical solution in the direction normal to the flow, as is shown in Fig. 6A. In Fig. 6B, which shows the numerical solution obtained using the grid of Fig. 5B, it is shown that excessive numerical diffusion occurs due to crossflow diffusion. In both cases results for both  $10 \times 10$  cell

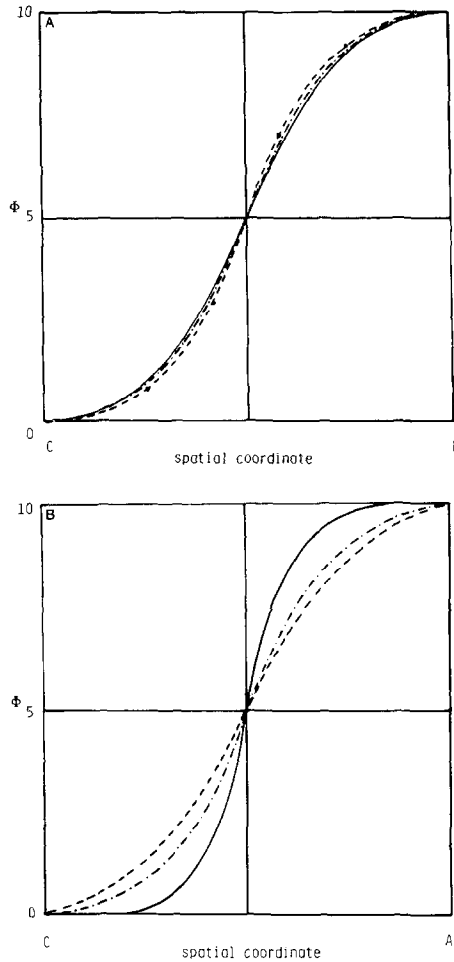


FIG. 6. (A) Comparison of the  $\Phi$ -distribution along the line  $CD$  in Fig. 5A from the analytic and numerical solutions, respectively, with donor cell differencing of the convective term using  $6 \times 6$  and  $10 \times 10$  grids. (B) Comparison of the  $\Phi$ -distribution along the line  $CA$  in Fig. 5B from the analytic and numerical solutions, respectively, with donor cell differencing of the convection using  $6 \times 6$  and  $10 \times 10$  grids. (Analytical solution (-); Numerical solution for  $6 \times 6$  (---) and  $10 \times 10$  (-.-).)

and  $6 \times 6$  grids are shown. The crossflow diffusion constant is proportional to the mesh spacing in Eq. (23), therefore more diffusion is observed in the coarser grid solutions.

#### Quantification of $D_{CF}$

To demonstrate the correct quantification of the crossflow diffusion error, results from the two formulae for the prediction of crossflow diffusion, Eqs. (14) and (23), are presented. They yield the same crossflow diffusion coefficient for the case of

$\theta = \theta_1 = 45^\circ$  where  $\theta = \tan^{-1} v/u$  and  $\theta_1 = \tan^{-1} \Delta y/\Delta x$ . The problem geometry in Fig. 7 has the arbitrarily chosen angles of  $\theta$  and  $\theta_1$  of  $60$  and  $76.81^\circ$ , respectively. Figure 8 shows the comparisons for the  $\phi$ -distribution along the line  $BD$  of Fig. 7 of the numerical solutions and the analytical solution with the diffusion constant  $(A)(D + D_{CF})$ , where the crossflow diffusion constant  $D_{CF}$  is given by Eq. (23) and  $(B)(D + D_{DM})$  when  $D_{DM}$  is given by Eq. (14). Superiority of the prediction formula Eq. (23) is indicated by the observation that agreement of the analytical solution with the former treatment is better than the latter.

Application of the new crossflow diffusion corrective scheme to a standard problem:

The corrective scheme proposed in this paper is applied to the test problem illustrated in Fig. 9, where the inlet  $\phi$ -profile and the velocity field are prescribed,

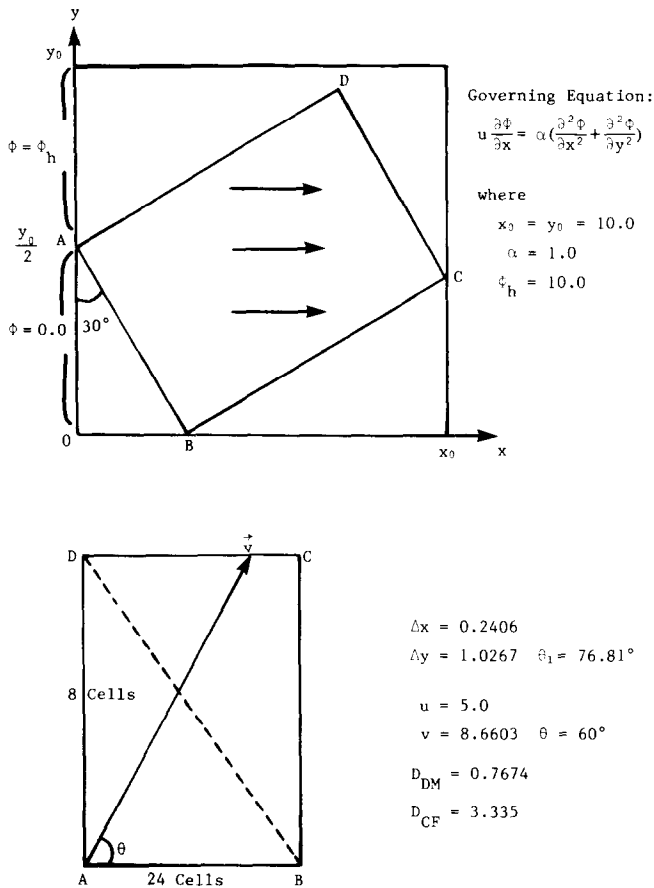


FIG. 7. Problem geometry with arbitrary values of  $\theta$  and  $\theta_1$  to compare results from Eqs. (14) and (23) for prediction of crossflow diffusion coefficient.

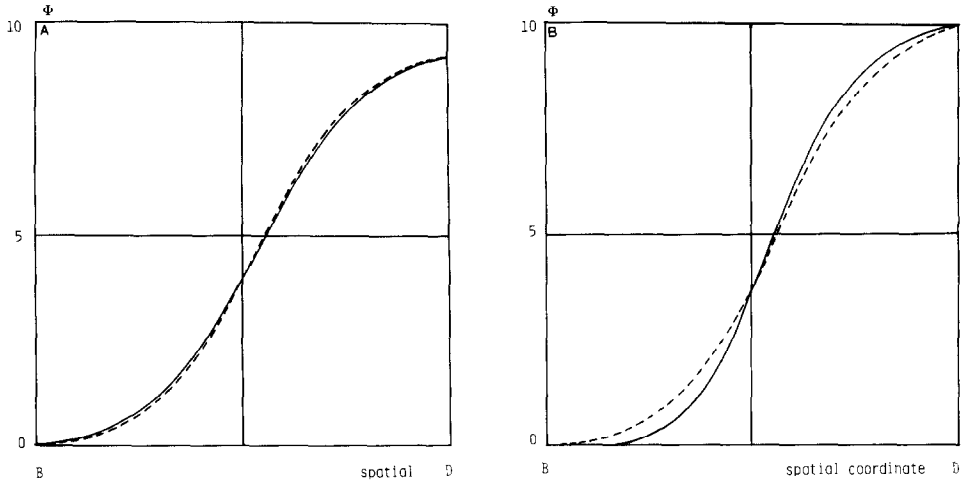


FIG. 8. Comparison of the  $\Phi$ -distributions along the line  $BD$  for the flow illustrated in Fig. 7 from the numerical solution (---) using donor cell differencing and analytic solutions (-) using diffusion coefficients increased to include crossflow diffusion terms: (A)  $D_e = D + D_{CF}$ ,  $D_{CF}$  from Eq. (23), (B) ( $D_e = D + D_{DM}$ ,  $D_{DM}$  from Eq. (14).

Governing Equation:

$$\vec{v} \cdot \nabla \phi - \frac{1}{Pe} \nabla^2 \phi = 0$$

Velocity field:

$$u = 2y(1 - x^2)$$

$$v = -2x(1 - y^2)$$

Boundary condition:

$$\phi = 1 + \tanh[(2x+1)\alpha]$$

$$y = 0, -1 \leq x \leq 0 \text{ (inlet)}$$

$$\phi = 1 - \tanh \alpha$$

$$\begin{cases} x = -1, 0 \leq y \leq 1 \\ y = 1, -1 \leq x \leq 1 \\ x = 1, 0 \leq y \leq 1 \end{cases}$$

where  $\alpha = 10.0$

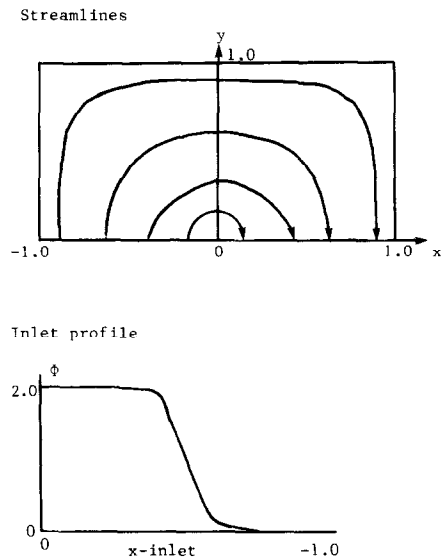


FIG. 9. Geometry and flow of test problem for numerical representation of convection, from [12].





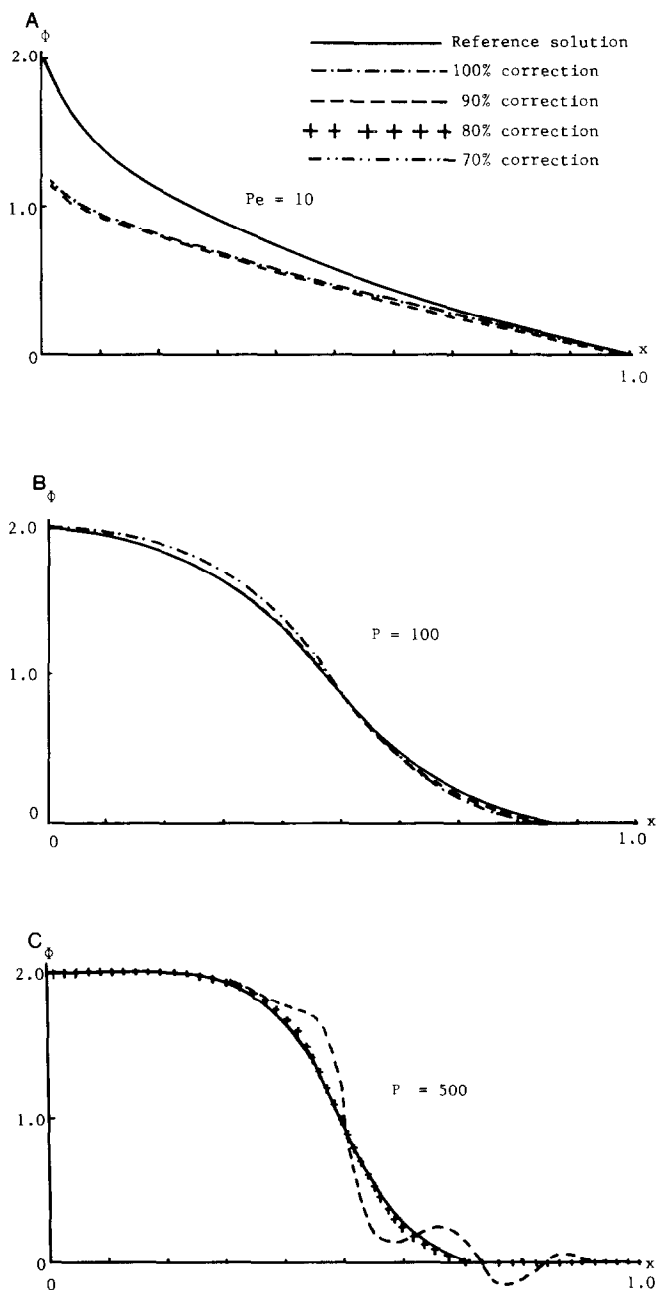


FIG. 10. Comparison of reference solution to numerical solutions using proposed corrective scheme: (A)  $P = 10$ , (B)  $P = 100$ , (C)  $P = 500$  (D)  $P = 10^3$ , and (E)  $P = 10^6$ . (Reference solution (-); 100% correction (-·-·-); 90% (- - -); 80% (+ + +); 70%(-·-·-).)

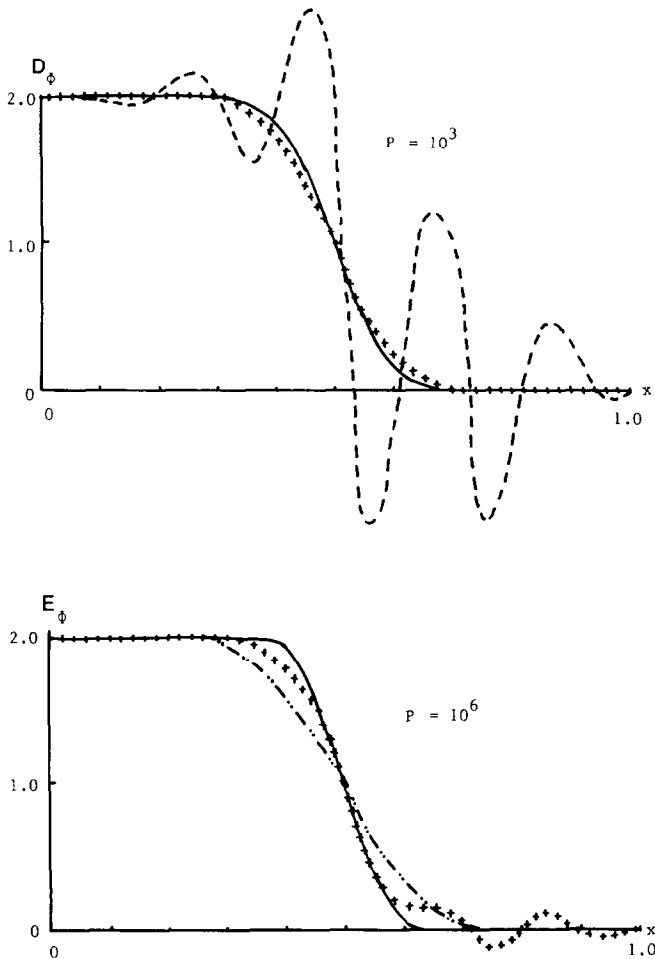


FIG. 10—Continued.

0.9  $D_{CF}$ ) is almost identical to the reference solution. For  $P = 500$  and  $P = 1000$ , the solution with 80% correction yields the best results. Although the quality of the results degrades slightly for larger Peclet numbers, good agreement between the reference and numerical solution continues to be obtained. For  $P = 10^6$ , the solution with an 80% correction shows an oscillating tail near the boundary region while the solution with a 70% correction shows excessive diffusion without oscillation. As larger diffusion corrections are made, more deviation occurs between the reference and numerical solution due to this oscillation. The cause of the oscillation is the existence of a negative net diffusion coefficient,  $(D_{ph} + D_{ND} - D_{CF})$ , occurring within the domain. In a convection-dominant problem the physical diffusion coefficient  $D_{ph}$  is much smaller than the numerical

and crossflow diffusion coefficients  $D_{ND}$  and  $D_{CF}$ . Therefore the net diffusion coefficient may become negative when the crossflow diffusion coefficient  $D_{CF}$  is slightly overpredicted. Prediction of the crossflow diffusion coefficient  $D_{CF}$  by Eq. (23) should be accurate in a unidirectional flow, but may be in error when the flow changes its direction continuously because the change of flow direction over one mesh spacing is not taken into consideration in the derivation of the corrective scheme.

The crossflow diffusion coefficients which obtain for this problem are listed in Table III. It is seen that  $D_{CF_x}$  and  $D_{CF_y}$  attain their greatest values in the regions of the domain where the angle between the velocity and  $\alpha$  axis is close to  $45^\circ$ . For this problem  $D_{ph} \approx 1/p$ . Difficulties would be encountered in use of the convective scheme of this paper when  $D_{ph} \ll D_{CF}$  because of possible overconvection of numerical diffusion. Since  $D_{CF_{max}} = 0.035$  it would be expected that the convective scheme would work well for values of  $P < 100$ , and would exhibit possible overconvection at greater values of  $P$ .

The partial corrections used in this example illustrate the limitations of the corrective scheme. Such behavior is observed in this example with oscillatory solutions being observed earliest as  $P$  increases in the regions where  $D_{CF}$  is large. A calculation exhibiting oscillatory solutions such as those shown here may need to be performed again using a reduced correction in order to obtain stable results. Sources of possible overcorrection include numerical errors in addition to those of crossflow diffusion and incorrect evaluation of  $D_{CF}$  arising from nonuniformity in the velocity field over the space of a single cell.

## 7. CONCLUSIONS

The major conclusions of this article are the following:

(1) There are two numerical diffusion sources: truncation error and crossflow diffusion. Truncation error occurs due to use of approximate profile assumptions while crossflow diffusion occurs with the donor cell treatment of convection in a multidimensional problem. Truncation error diffusion causes negligible errors in both diffusion-dominant and convection-dominant problems whereas crossflow diffusion causes significant errors in multidimensional convection-dominant problems. Consequently crossflow diffusion is the dominant error that should be corrected for acceptable solution accuracy in most fluid dynamic problems of practical interest.

(2) Two types of approaches for elimination of the crossflow diffusion error, skew upwind-differencing and corrective schemes, have been used widely. The skew upwind differencing scheme gives good results for some problems, but may give unphysical results in recirculating flow problems using coarse grids. The corrective scheme presented in this work is based on the fact that crossflow diffusion can be predicted accurately for every mesh at every time-step. Stability analysis shows that

there exists a stable range of the time-step size for a certain negative range of the cell Peclet number.

(3) The corrective scheme gives satisfactory results for most convection-diffusion problems. However, for certain cases characterized by high Peclet numbers and substantial curvature of the velocity field over a single mesh spacing, unphysical oscillations in the numerical solution may arise. Slight overprediction of the crossflow diffusion constant  $D_{CF}$  can render the net diffusion constant,  $(D_{ph} + D_{ND} - D_{CF})$ , negative when the physical diffusion constant  $D_{ph}$  is much smaller than the numerical and crossflow diffusion constants  $D_{ND}$  and  $D_{CF}$ . Once the net diffusion constant becomes negative, the resulting numerical solution exhibits an oscillation which degrades the solution accuracy very rapidly.

#### ACKNOWLEDGMENTS

The authors gratefully acknowledge the research support of the Boston Edison Co., Duke Power Corp., Northeast Utilities Service Corp., and Public Service Electric and Gas Co. of New Jersey.

#### REFERENCES

1. B. R. BALIGA AND S. V. PATANKAR, *Numer. Heat Transfer* **3** (1980), 393.
2. S. H. CHANG, "Comparative Analysis of Numerical Methods for the Solution of the Navier-Stokes Equations," MIT Ph.D. thesis, Cambridge, Mass., 1981.
3. G. DEVAHL DAVIS AND G. D. MALLINSON, *Comput. and Fluids* **4** (1976), 29.
4. J. K. DUKOWICZ AND J. D. RAMSHAW, *J. Comput. Phys.* **32** (1979), 71.
5. J. E. FROMM, *J. Comput. Phys.* **3** (1968), 176.
6. C. W. HIRT, *J. Comput. Phys.* **2** (1968), 339.
7. S. V. PATANKAR, "Numerical Heat Transfer and Fluid Flow," Hemisphere, Washington, D.C., 1980.
8. G. D. RAITHBY AND K. E. TORRANCE, *Comput. and Fluids* **2** (1974), 191.
9. G. D. RAITHBY, *Comput. Methods Appl. Mech. Eng.* **9** (1976), 153.
10. P. J. ROACHE, "Computational Fluid Dynamics," Hermosa, Albuquerque, N. M., 1976.
11. P. J. ROACHE, *J. Comput. Phys.* **10** (1979), 169.
12. R. M. SMITH AND A. G. HUTTON, *Numer. Heat Transfer* **5** (1982), 411.
13. D. B. SPALDING, *Int. J. Numer. Methods Eng.* **4** (1972), 551.
14. G. D. STUBLEY, G. D. RAITHBY, AND A. B. STRONG, *Numer. Heat Transfer* **3** (1980), 411.
15. G. D. STUBLEY, G. D. RAITHBY, A. B. STRONG, AND K. A. WOLNER, *Comput. Methods Appl. Mech. Eng.* **35** (1982), 153.